NASA TECHNICAL MEMORANDUM

NASA TM-77999

INFRARED DIAGNOSIS USING LIQUID CRYSTAL DETECTORS

Hugenschmidt, M., Vollrath, K.

NASA-TM-77999 19860012344

Translation of "Infrarotdiagnostik mit Hilfe von Flüssigkristalldetektoren," Bundesministerium der Verteidigung, Forschungsbericht aus der Wehrtechnik BMVg-FBWT 73-16, 28 pp.

NATIONAL AERONAUTICS AND SPACE ADMINISTRATION
WASHINGTON, D.C. 20546 FEBRUARY 1986

STANDARD TITLE PAGE

1. Report No.	2. Government Accession No.	3. Recipient's Catalog No.
NASA TM-77999		

4. Title and Subtitle	5. Report Date
INFRARED DIAGNOSIS USING LIQUID CRYSTAL DETECTORS	6. Performing Organization Code

7. Author(s)	8. Performing Organization Report No.
Hugenschmidt, M., Vollrath, K. Institut Franco-Allemand de Recherches	10. Work Unit No.

9. Performing Organization Name and Address	11. Contract or Grant No.
Leo Kanner Associates, Redwood City, California 94063	NASw- 4005
	13. Type of Report and Period Covered
12. Sponsoring Agency Name and Address	Translation
National Aeronautics and Space Administration, Washington, D.C. 20546	14. Sponsoring Agency Code

15. Supplementary Notes

Translation of "Infrarotdiagnostik mit Hilfe von Flüssigkristalldetektoren," Bundesministerium der Verteidigung, Forschungsbericht aus der Wehrtechnik BMVg-FBWT 73-16, 28 pp.

16. Abstract

The possible uses of pulsed carbon dioxide lasers for analysis of plasmas and flows need appropriate infrared image converters. Emphasis was placed on liquid crystal detectors and their operational modes. Performance characteristics and selection criteria, such as high sensitivity, short reaction time, and high spatial resolution.

17. Key Words (Selected by Author(s))	18. Distribution Statement
	Unclassified - unlimited

19. Security Classif. (of this report)	20. Security Classif. (of this page)	21. No. of Pages	22.
Unclassified	Unclassified		

INFRARED DIAGNOSIS USING LIQUID CRYSTAL DETECTORS

Hugenschmidt, M., Vollrath, K.
Institut Franco-Allemand de Recherches, St. Louis

/III*

Abstract

The possibility of applying pulsed CO_2 lasers, particularly using the TEA principle, for plasma or flow diagnosis, requires appropriate infrared image converters. In addition to visualizing radiation by thermal extinction of UV-activated fluorescent layers, liquid crystal detectors are very important here.

The structure and performance of various detectors are described, with special emphasis on their suitability as to high sensitivity, fast response and maximum spatial resolution.

---

*Numbers in the margin indicate pagination in the foreign text.

Contents /0

Introduction

/1

To visualize infrared radiation, a number of partially reversible physical processes exist, including Czerny evaporography, thermal melting or sublimation, effects of chemical reactions on photochromic layers, extinction of fluorescence and the use of cholesterol liquid crystals. The last procedure is discussed in detail below. These methods are interesting since infrared light sources are used in plasma physics. Moreover, there are numerous fields of application in medicine, geography and non-destructive materials testing, as well as quite generally in the field of short-time physics. In particular, short-time photography and cinematography are concerned with opening a broader range of the spectrum besides the previous emission light sources in the X-ray range, UV, visible and near infrared.

The present paper examines the properties and behavior of cholesterol liquids, primarily with regard to their suitability for recording rapidly changing processes, using a TEA laser as a short-time infrared light source.

TEA Laser

A transversely excited CO_2 laser was used at atmospheric pressure, as first developed by Beaulieu and similarly used by Büchl to generate and heat hydrogen and deuterium plasmas [1,2].

The laser is almost 4 m long and at a maximum pulse repetition frequency of 40 Hz (for slowly flowing gas) it emits pulses with an energy of 0.3 to 0.5 J and a half-amplitude duration of 0.2 to 0.3 μs.

Figure 1 shows a diagram of the produced laser and an oscillogram of the course of the output pulse over time, measured with a Ge-Au detector. This involves superimposing 10 individual

pulses. The reproducibility is excellent.

/2

Figure 2 shows the specific structure of the resonator with a plane-convex Ge lens (focal length f = 20 cm) as a catcher reflector, as well as the transverse intensity distribution before the focal plane at A-B and C-D.

Developed Polaroid film was used for recording. The power density is sufficient to provide a good picture of transverse distribution. The spatial resolution achieved by this simple method, as also measured by Därr, Decker and Röhr, is 20 lines per mm. But the sensitivity is no longer adequate for a greatly expanded beam, such as is required to illuminate larger surface areas [3].

Liquid Converters

In liquid crystals, a distinction is made between smectic and nematic phases, which possess thread-shaped molecules in essentially parallel orientation. Cholesterol liquids, however, consist of flat asymmetric molecules which are parallel in each layer but rotated at a certain angle from one layer to the next. Such layers present a high optical activity. The effect used in the present paper arises from the fact that this periodic layering and its temperature dependency produces a strong dependency on direction and frequency, particularly of the back-scattered light. Measurements are performed with a mixture of cholesterol oleyl carbonate and nonoate (85:15). This solution is sprayed homogeneously, with a layer thickness of a few μm, onto thin absorbent films which themselves are only a few 10 μm thick. A drawback is that in the open atmosphere one observes an aging process attributable primarily to contaminants and humidity. Therefore, each layer must be replaced every few days. This drawback disappears when one uses liquid crystals from NCR, which are delivered in micro-encapsulated form.

Films of Rhodialine, Vynan and homemade films of polyvinyl alcohol with colloidal graphite were studied as supports for liquid crystals. The intensity absorption coefficients of these materials were between 1.3×10^2 and 7.5×10^2 cm^{-1}. If one /3 requires the greatest possible absorption, e.g. greater than 98%, this yields minimum necessary layer thicknesses of 50 to 300 μm. Most measurements were performed with Vynan films 40 μm thick from the "La Cellophane" company.

Figure 3, as a first example, shows two photos: A recording of transverse intensity distribution with and without a diaphragm in the far field of the expanded beam.

Sensitivity, Response Time and Resolution

For short-time photography applications, the essential parameters are sensitivity, response over time and spatial resolution.

Assuming a layer with a color change interval of 1 to 2°C (from red to blue), an energy density of 4 mJ/cm^2 is necessary for a temperature increase of 0.3 to 0.5°C that is sufficient for good color contrast, given a total layer thickness of 40 μm and a mean specific heat of 0.34 cal/°C g.

To reduce the influence of thermal conductivity, the temperature distribution characterized by color changes should be photographed as soon as possible after impingement of the CO_2 laser.

Figure 4 shows the measurement setup and some results. It indicates a recognizable color change after only 5 ms. Subsequently the contrast increases, and at the relatively late time of 50 ms a thermal diffusion of the initial distribution is

already noted. The superimposition of two interference schlieren systems was chosen as an example: Concentric circles provoked by the uncoated catcher lens, and parallel strips due to transmission through a Ge plate with a small wedge error. /4

Figure 5 shows another example: As shown schematically in the lower half of the figure, these are shadow photographs of an electrical spark discharge, recorded 1 μs after arc-through. As the photographs show, at this early point the plasma is still opaque to the radiation of the CO_2 laser, so that both the spark channel and the areas shaded by the electrodes present a reflection maximum in the red range. These sample photos also show that the employed crystals require a time of 5 to 10 ms to develop adequate schlieren contrast. Within this time, heat transport mechanisms can already play a significant role.

This influence was studied numerically from a simple model, shown in Fig. 6. A one-dimensional treatment is possible, since the layer depth is negligible compared to the lateral dimensions. Taking the initial and boundary conditions into account, for a $\cos^2$ initial temperature distribution one gets a solution shown in Fig. 6.

Λ is the schlieren separation. For the thermal conductivity a^2, with the data for Vynan, one gets a value of 1.13×10^{-3} cm^2/s.

Two examples of the decay of the temperature distribution are shown in Fig. 7. For Λ = 0.1 mm, i.e. a resolution of 10 lines per mm, a sharp decay of schlieren contrast occurs within a few seconds.

Resulting from a number of further calculations, Fig. 8 shows the decay of schlieren contrast over time. These calculations show that because of the relatively slow liquid crystal

response time of 5 to 10 ms, with the present setup the upper limit of achievable resolution is set by the steep drop in the contrast factor K. This value is 5 to 10 lines per mm.

Application of Optical Infrared Methods

As the measurements and calculations described above show, such liquid crystal image converters permit the application of a number of different optical procedures. This will be shown from a few examples.

Figure 9 contains three photos of electrical spark discharges. The recording times are 1 to 2 μs after arc-through. The capacity of the discharge circuit is 0.02 μF, the charge voltage is 7.5 kV and the electrode gap is 2.5 mm. The photographs show the shaded areas of the spherical electrodes and the discharge channel, which has already achieved a diameter of 1.2 to 1.4 mm.

To reduce the maximum current, the discharge circuit was attenuated with an additional 10 Ω resistor. It is interesting that in these photographs the outer edge zone of the plasma is still opaque for 10 μm because of the greater geometric layer depth, while the inner area is already becoming transparent.

Further photographs at a somewhat later point are shown in Fig. 10. With the same electrical data, here the channel diameter in the first picture on the left is already 2.1 mm. The two photos on the right were obtained using a schlieren technique.

For this the experimental setup was slightly modified by applying a schlieren edge in the shared focal plane of the beam expansion system.

Besides these examples, which only supply qualitative information about refractive index gradients, Fig. 11 also contains two photos: interferograms recorded using an infrared Michelson interferometer.

Such interferograms allow direct quantitative statements about refractive index distribution and thus about further variables of state, especially electron density. /6

Conclusions

The described measurements and calculations show that liquid crystal layers are suitable for recording quickly changing phase objects, using CO_2 laser pulses.

The maximum spatial resolution of the studied setup, determined by the finite rise time, is 10 lines per mm. By contrast, for holographic applications resolutions of 150 to 200 lines per mm would be needed.

On the other hand, liquid crystal detectors allow excellent optical recording by conventional methods, such as:

-- the schlieren and shadow method or

-- by interferometry.

REFERENCES

[1] J.A. Beaulieu, "High peak power gas lasers," Proceedings of the IEEE 59 (1971), 667.

[2] K. Büchl, "Production of Plasma with a CO_2-TEA Laser from Solid Hydrogen Targets," Max-Planck Institut für Plasmaphysik, Garching, IPP IV/16 (1971).

[3] A. Därr, G. Decker, H. Röhr, "Side on interferometry at 10.6 μm of theta pinch plasmas," Z. Physik 248 (1971), p. 121.

Fig. 1. Diagram of TEA laser, curve of coupled pulses over time.

Key: a. relative intensity b. ges = total
c. Ge-Au detector

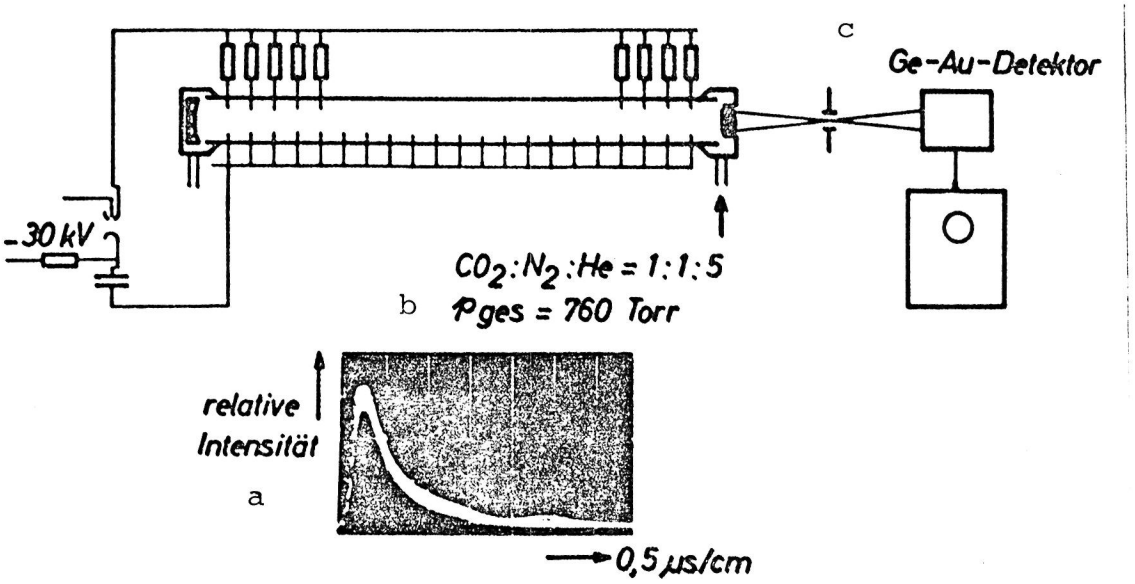

Fig. 2. Structure of the resonator and beam expansion system, and transverse intensity distribution.

Key: a. steel reflector b. Ge lens c. diaphragm
d. transverse intensity distribution in plane ...

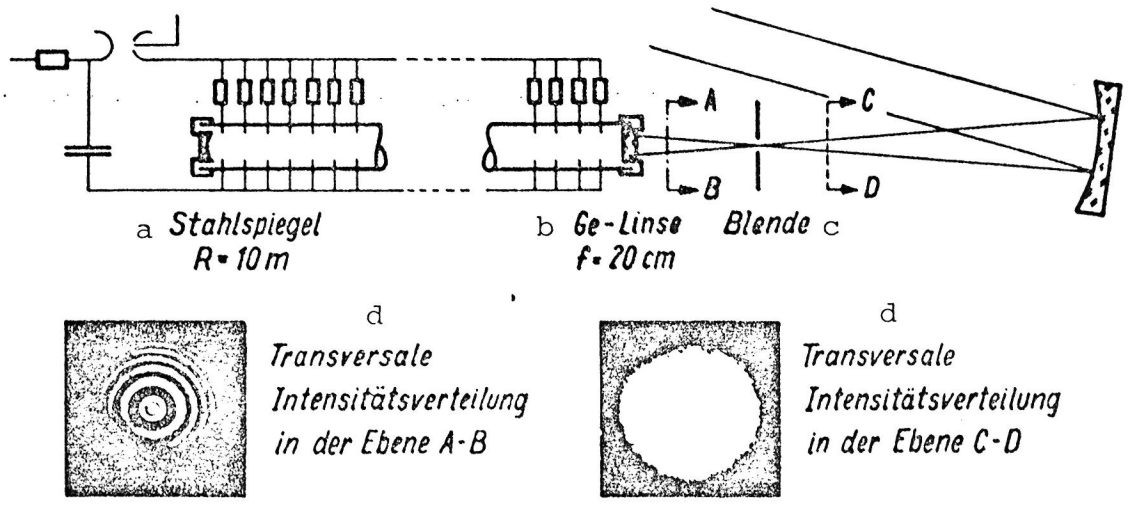

/9

Fig. 3. Photographs of transverse intensity distribution of TEA laser pulses a) without and b) with diaphragm in the focal plane of the confocal beam expansion system. Recording with a liquid crystal image converter.

Key: c. stop d. liquid crystal layer

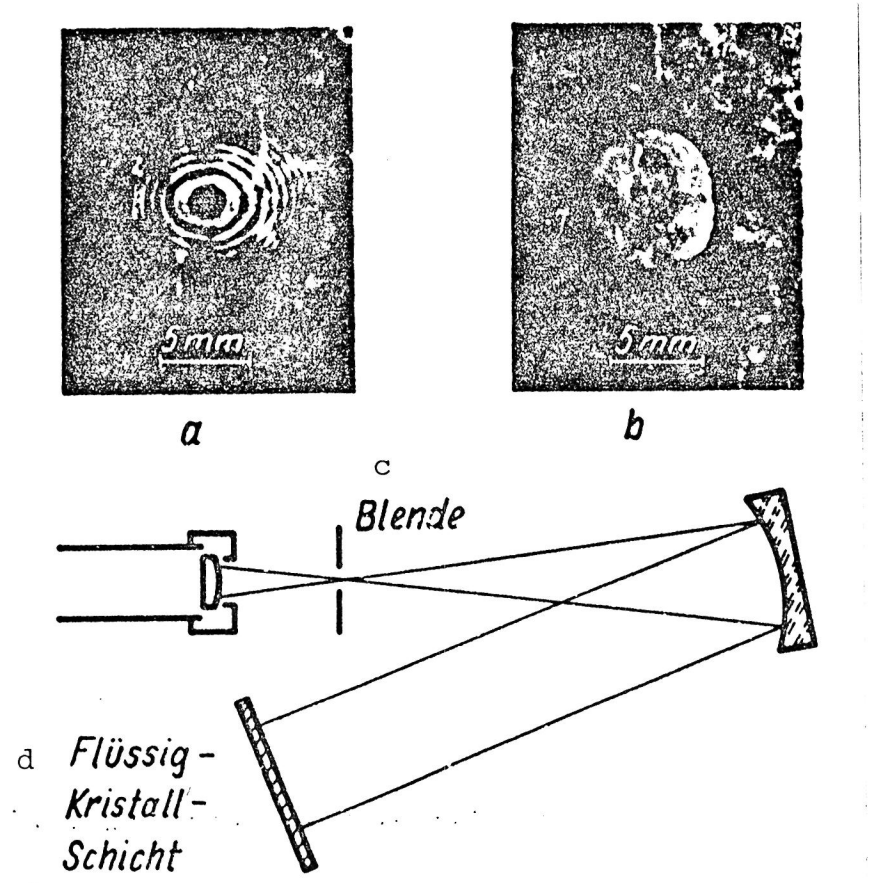

/11

Fig. 4. Measurement of response time of liquid crystal layer. The parameter is the delay time Δt for turning on the flash lamp. (The photographs show the superimposition of two interference schlieren systems after transmission through a Ge plate.)

Key: a. Ge plate b. liquid crystal layer
c. flash lamp

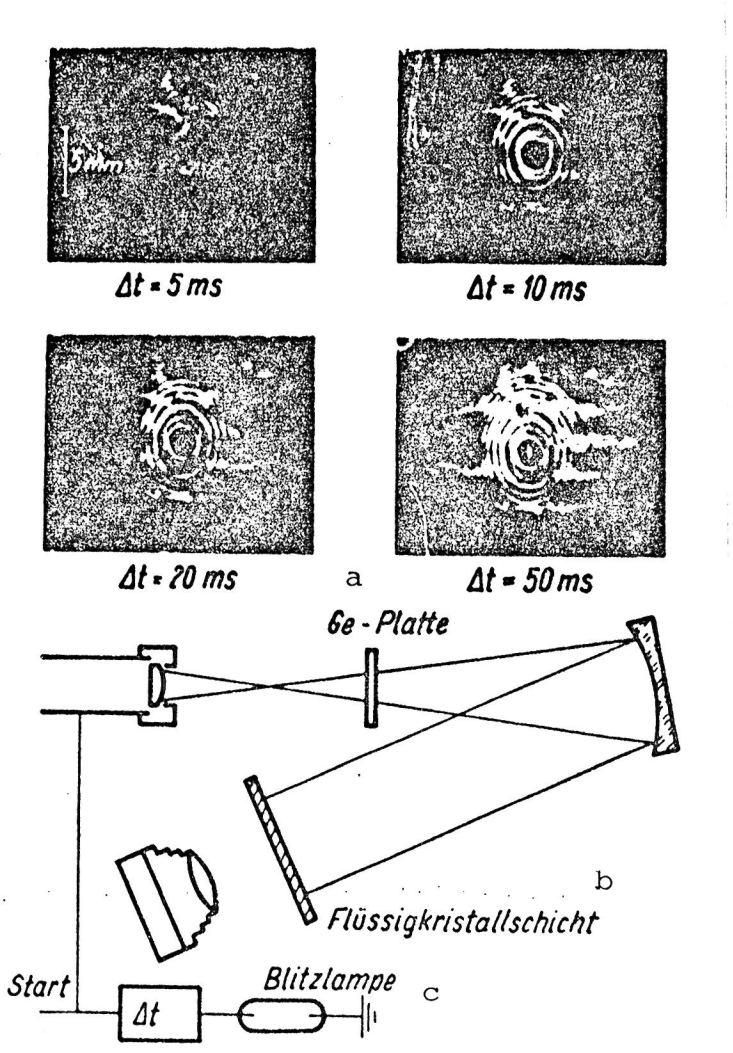

Fig. 5. Time response, shown from the example of shadow photographs of an electric spark discharge.
Channel stage: 1 μs after initiation
Parameter: Delay time Δt for triggering the flash lamp

Key: a. liquid crystal layer b. flash lamp

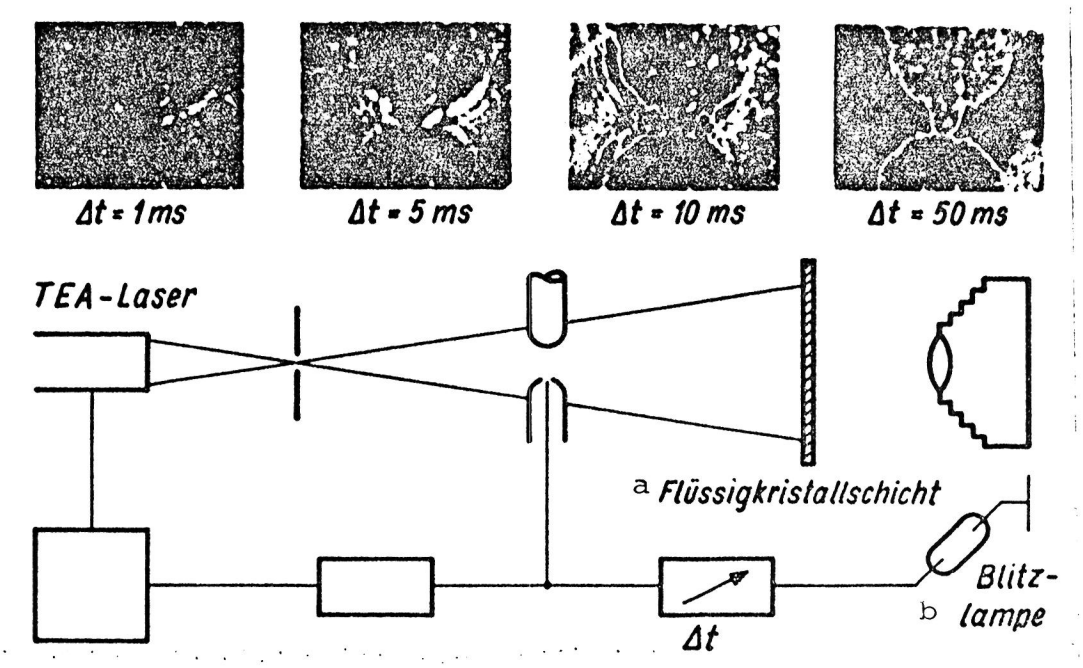

/15

Fig. 6. Solution of heat conduction equation for a thin film in the case of a $\cos^2$ initial temperature distribution.

Heat conduction in a thin film

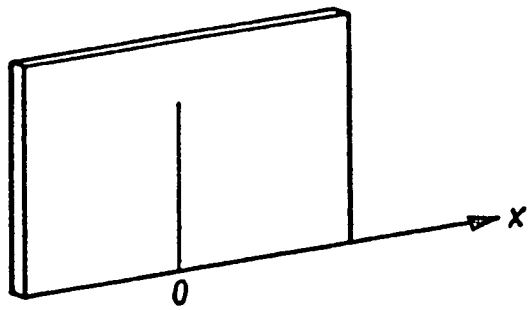

General heat conduction equation
a^2 = thermal conductivity

$$\frac{\partial \vartheta}{\partial t} - a^2 \Delta \vartheta = F(x,t)$$

Solution for the one-dimensional case of a homogeneous equation for a periodic initial temperature distribution

$$\vartheta_K(x,t) = X_K(x) \cdot T_K(t)$$

$$\vartheta(x,t) = \sum_K A_K \cos Kx \, e^{-K^2 a^2 t}$$

$\cos^2$ initial temperature distribution

Initial condition
Λ = schlieren separation

$$\vartheta(x,0) = \vartheta_0 \cos^2 \frac{\pi x}{\Lambda}$$

Boundary condition

$$\left.\frac{\partial \vartheta}{\partial x}\right|_{x=0} = 0$$

$$\vartheta(x,t) = \frac{\vartheta_0}{2}\left[1 + \cos \frac{2\pi x}{\Lambda} \, e^{-\frac{4\pi^2}{\Lambda^2} a^2 t}\right]$$

Data for Vynan:

Thermal conductivity	λ	$5 \cdot 10^{-4}$	$\left[\frac{cal}{cm\,s\,^\circ C}\right]$
Specific heat	c	0,34	$\left[\frac{cal}{g\,^\circ C}\right]$
Specific gravity	γ	1,3	$\left[\frac{g}{cm^3}\right]$

$$a^2 = \frac{\lambda}{c \cdot \gamma} = 1{,}13 \cdot 10^{-3} \left[\frac{cm^2}{s}\right]$$

Fig. 7. Spatial temperature distribution at different times, based on a $\cos^2$ initial temperature distribution. Parameter: Schlieren separation Λ. /17

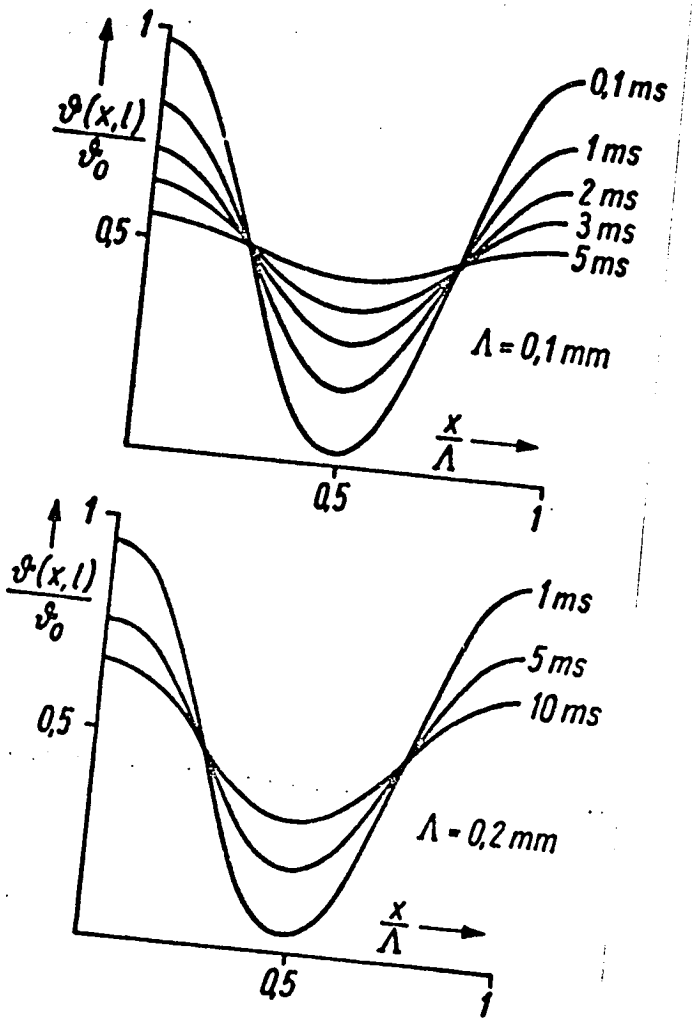

Fig. 8. Decay of schlieren contrast over time. Parameter: schlieren separation Λ.

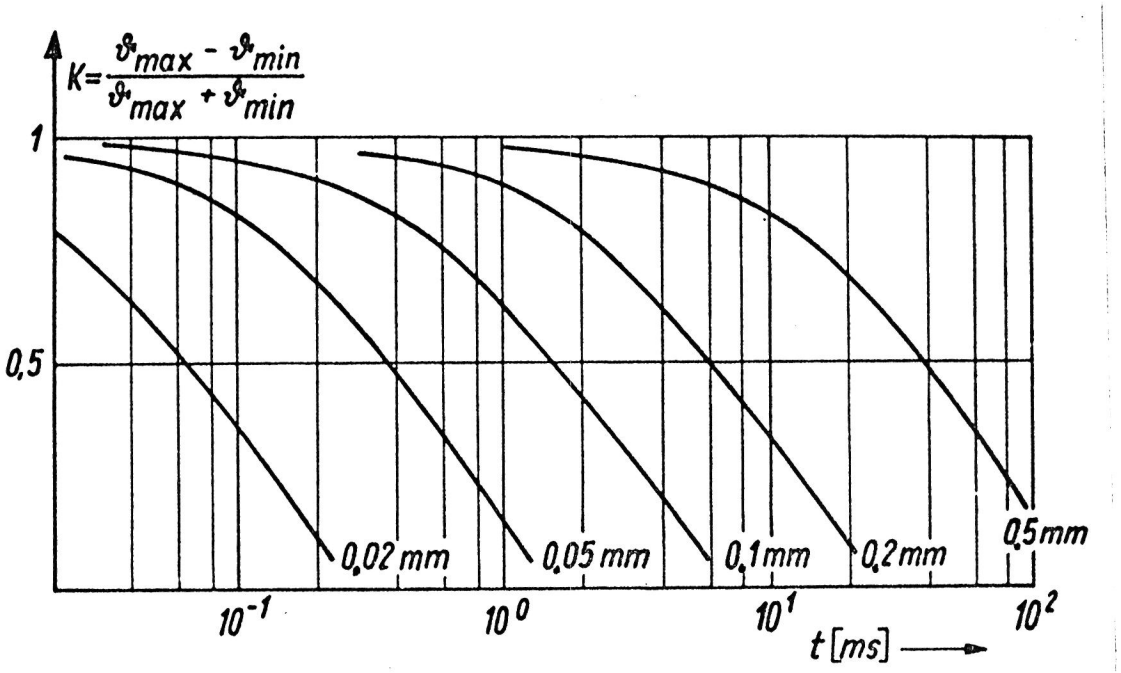

Fig. 9. Infrared shadow photographs of electric spark discharges.
C = 0.02 μF, U = 7 kV, electrode separation d = 2.5 mm
Time stages of discharge ca. 1 to 2 μs after initiation.

/21

Fig. 10. a) Infrared shadow photograph and b,c) schlieren photographs of late stages of electric spark discharges, 4 to 15 μs after initiation.
C = 0.02 μF, U = 7 kV, electrode separation d = 2.5 mm

a) b) c)

Fig. 11. Interferograms of the late stage of an electric spark discharge, 20 μs after initiation.
Resolution of flash lamp: a) 15 ms, b) 50 ms, both after impingement of CO_2 laser on liquid crystal layer.

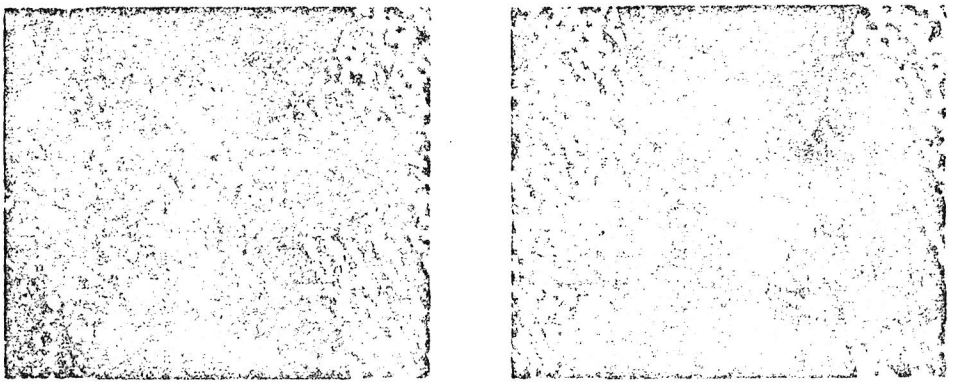

a) b)

DO NOT REMOVE SLIP FROM MATERIAL

Delete your name from this slip when returning material to the library.

NAME	MS

NASA Langley (Rev. May 1988) RIAD N-75